Two-dimensional stationary soliton gas

Thibault Bonnemain [1], Gino Biondini [2], Benjamin Doyon [1], Giacomo Roberti [3] and Gennady A. El [3,*]
[1] Department of Mathematics, King's College, London WC2R 2LS, United Kingdom
[2] Department of Mathematics and Department of Physics, State University of New York, Buffalo, New York 14260, USA
[3] Department of Mathematics, Physics and Electrical Engineering, Northumbria University, Newcastle upon Tyne NE1 8ST, United Kingdom

(Received 21 August 2024; accepted 3 December 2024; published 7 February 2025)

We study two-dimensional stationary soliton gas in the framework of the time-independent reduction of the Kadomtsev-Petviashvili (KPII) equation, which coincides with the integrable two-way "good" Boussinesq equation in the xy plane. This $(2+0)$D reduction enables the construction of the spatial analog of the kinetic equation for the stationary gas of KP solitons by invoking recent results on $(1+1)$D bidirectional soliton gases and generalized hydrodynamics of the Boussinesq equation. We then use the spectral kinetic theory to analytically describe two basic types of 2D soliton gas interactions: (i) refraction of a line soliton by a stationary soliton gas, and (ii) oblique interference of two soliton gases. We verify the analytical predictions by numerically implementing the corresponding KPII soliton gases via exact N-soliton solutions with N-large and appropriately chosen random distributions for the soliton parameters. We also explicitly evaluate the long-distance correlations for the two-component interference configurations. The results can be applied to a variety of physical systems, from shallow water waves to Bose-Einstein condensates.

DOI: 10.1103/PhysRevResearch.7.013143

I. INTRODUCTION

The concept of soliton gas (SG) as an infinite random ensemble of interacting solitons has recently emerged as a new and powerful tool for understanding nonlinear random wave fields in the language of statistical physics and hydrodynamics. It was first introduced for a rarefied, or dilute, gas of Korteweg-de Vries (KdV) solitons [1], then generalized to dense gases and other integrable dynamical models [2–5]. SGs have been observed in various physical media, including water waves [6–9], photorefractive crystals [10], and superfluids [11].

The theory of SGs relies on the integrability of the underlying nonlinear wave model and, in particular, on the tools of the inverse scattering transform (IST) that relate solitons to the discrete spectrum of the associated linear Lax operator [12,13]. In the IST formalism, a discrete eigenvalue associated to a soliton uniquely defines its amplitude and velocity. A key quantity in the SG theory is the density of states (DOS)—the joint distribution of solitons with respect to their spectral eigenvalues and positions in space. The DOS is a macroscopic characteristic of a SG defining the ensemble averages (observables) of the associated nonlinear random wave field, often called *integrable turbulence* [14].

For spatially nonuniform dense SGs the DOS evolution is determined by the kinetic equation [3], which can be interpreted as a continuity equation, where the flux density is determined by an integral equation of state that simply accounts for the average soliton velocity in the gas via a *collision rate ansatz*. The collision rate ansatz is obtained from two system-specific ingredients expressed in spectral terms: the free soliton velocity and the phase or position scattering shift. Soliton interactions are assumed to occur as sequences of two-body interactions, in agreement with two-particle factorisation of many-particle scattering. This is consistent with systematic spectral theory derivations for the KdV and focusing nonlinear Schrödinger (NLS) SG [2,4]. The predictions of the kinetic SG theory for the focusing NLS equation were successfully verified in fibre optics and deep-water tank experiments in [15,16]. We refer the reader to the recent reviews [17,18] for further theoretical and experimental developments.

The construction of SG kinetic equation in [3] is also consistent with the *generalized hydrodynamics* (GHD) approach [19–22], which has proven to be a powerful theoretical framework for the understanding of large-scale, emergent hydrodynamic properties of integrable quantum and classical many-body systems. The relation between the KdV and Boussinesq SG, and their GHD description, was recently established in [23,24], where the formulation of their *thermodynamics* and generalized Gibbs ensembles via the thermodynamic Bethe ansatz was also worked out.

The collision rate ansatz and GHD approaches make it clear that the theory can be adapted to many soliton and interaction types [25], including bidirectional dispersive wave systems exhibiting anisotropic soliton collisions, where phase shifts in overtaking and head-on interactions are different, e.g., see [26]. In this case one obtains a coupled system

*Contact author: gennady.el@northumbria.ac.uk

of two kinetic equations for different types of solitons [5]. This has important implications for the behavior of the physical wave field in a SG. Various physical systems exhibit anisotropic soliton interactions [27,28] whose generic properties are acutely captured by the classical integrable two-way Boussinesq equation [29].

Virtually all works on SGs so far were limited to one spatial dimension, with the recent exceptions of [9], where an experimental observation of 2D shallow water SG was reported and [30] reporting the observation of 2D SG in a photon fluid. In this paper we provide a first step towards the analytical description of the emergent hydrodynamics of a two-dimensional SG, by describing the *spatial statistics of a time-stationary but nonhomogeneous gas*. We do so in the framework of the Kadomtsev-Petviashvili (KP) equation [31], the generalization of the KdV equation to weakly two-dimensional nonlinear dispersive waves [12] with applications to a broad variety of physical settings: from shallow water waves and plasma physics [32,33] to ferromagnetism and Bose-Einstein condensates [34–37]. The KP equation arises in two versions, called KPI and KPII, both integrable and possessing line soliton solutions [38–42]; we concentrate on KPII, whose solitons are stable and which has broader physical relevance. The SG studied in this paper is thus a "gas of lines" in contrast to the "gas of particles" in the conventional 1D SG theory.

Our results are based on the observation that the Galilean-boosted KPII equation admits a time-stationary reduction that coincides with the integrable "good" Boussinesq equation [43] in which the Boussinesq time y is one coordinate of the KP spatial xy plane. Trajectories of Boussinesq solitons correspond to KPII line solitons. Hence, a $(1+1)$D SG for the Boussinesq equation is mathematically equivalent to a stationary (or propagating with constant velocity) $(2+0)$D line SG of the KPII equation.

The correspondence between 2D stationary problems and 1D evolutionary ones is widely used in classical gas dynamics, where the methods of 1D hyperbolic conservation laws theory are employed to describe 2D steady wave structures such as oblique shock and expansion waves in supersonic flows past obstacles [44–46]. More recently, this correspondence was used to describe stationary oblique solitons and dispersive shock waves in the context of the nonlinear Schrödinger equation [47–49]. Note that in all previous studies the $(1+1)\text{D} \mapsto (2+0)\text{D}$ mapping was used to describe deterministic wave structures. In this paper, we take advantage of the equivalence between the stationary KPII equation and the evolutionary integrable two-way Boussinesq equation to describe the *spatial statistics* of the steady state nonlinear wave field in 2D soliton gases.

We leverage the recently developed kinetic theory of bidirectional anisotropic SGs [5] and the GHD theory for the Boussinesq equation [24], and infer some important implications for the respective 2D stationary gas of line KPII solitons. Specifically, we introduce and study analytically the phenomena of the line soliton refraction by a 2D SG and of the spatial interference of two SGs.

We verify the kinetic theory predictions numerically by constructing the corresponding KP and Boussinesq SGs via N-soliton solutions [39,42,50,51] with large N and appropriately chosen random distributions for the soliton parameters. Finally, we compute the spatial correlations for stationary two-component KP SGs.

II. KP AND BOUSSINESQ EQUATIONS, LINE SOLITON SOLUTIONS AND THEIR INTERACTIONS

The Galilean-boosted, dimensionless KPII equation reads (see Appendix A),

$$(u_t - u_x + 6uu_x + u_{xxx})_x + u_{yy} = 0. \tag{1}$$

Time-independent solutions of the above equation satisfy the so-called "good" Boussinesq equation

$$u_{yy} - u_{xx} + 3(u^2)_{xx} + u_{xxxx} = 0. \tag{2}$$

Equation (1) admits a two-parameter family of line-soliton solutions

$$u(x, y, t) = 2a^2 \operatorname{sech}^2[a(x - cy - vt) + \theta_o], \tag{3}$$

where θ_o is an arbitrary constant, and the soliton speed is completely determined in terms of the amplitude parameter a and the slope parameter c by the soliton dispersion relation $v = 4a^2 + c^2 - 1$. If $c = \pm\sqrt{1-4a^2}$, the above solution is stationary and is also a solution of the Boussinesq Eq. (2). This implies that (i) solitons of the Boussinesq equation cannot exceed the "speed of sound" $c = \pm 1$ in either direction of propagation, and (ii) their amplitude must be smaller than $a = 1/2$, which is only reached when $c = 0$. Note that the above relation determines the slope c up to a sign, Eq. (2) is a bidirectional model. In addition, both the KPII and Boussinesq equations admit a large family of (line-)soliton solutions, describing elastic interactions among individual solitons. These solutions are conveniently expressed via the Wronskian formalism [39,42,50–52], see Appendix A for details. One can view a as the *spectral parameter* of a line soliton (indeed, in the KdV and NLS inverse scattering formalism, the soliton amplitude is directly related to the discrete spectrum of the Lax operator [12,13]).

Interaction between solitons of the KPII equation leads to a shift in the position of each soliton as $y \to \infty$ compared to its position as $y \to -\infty$, and the same is true for the Boussinesq equation. Let $\varphi_{n,m}$ be the phase (position) shift of the nth soliton as a result of the interaction with the mth soliton. Two kinds of soliton interactions can occur depending on the relative sign of the slope of the individual solitons: (i) codirectional (co), when c_n and c_m have the same sign, and (ii) counterdirectional (ct), when c_n and c_m have opposite sign. Although in both cases the phase shift can be written as

$$\varphi_{n,m} = \frac{\operatorname{sgn}(a_m - a_n)}{2} \ln\left[\frac{(c_n - c_m)^2 - 12(a_n - a_m)^2}{(c_n - c_m)^2 - 12(a_n + a_m)^2}\right], \tag{4}$$

co- and counterdirectional interactions are phenomenologically different. In particular, since soliton amplitudes are positive and bounded by $1/2$, codirectional shifts are always negative, $\varphi^{\text{co}}_{n,m} < 0$, implying solitons effectively repel each other. Conversely, counterdirectional shifts $\varphi^{\text{ct}}_{n,m}$ can either be positive or negative depending on the relative amplitudes of the two solitons. This difference between the co- and counterdirectional phase shifts is naturally interpreted as anisotropy of soliton interactions [5]. Note that the logarithm in Eq. (4) implies that N-soliton solutions may develop resonances at finite values of y for certain sets of amplitudes. We restrict ourselves to regular solutions; conditions ensuring regularity at all time were first introduced in [53] and again discussed in [24]. Those conditions imply that no two solitons can have the same amplitude and that $\varphi_{n,m} \neq 0$ for admissible nonzero amplitudes.

III. KINETIC EQUATION FOR A 2D STATIONARY SG

Density of states (DOS) is the definitive characteristic of a SG that can be viewed as the density of soliton states in the spectral phase space at a given moment of time [17,18]. Given our choice of the spectral parameter a and following the general theory of bidirectional 1D SGs [5], we introduce the separate DOS's $f^{\mathrm{l}}(a;x,y)$ and $f^{\mathrm{r}}(a;x,y)$ for the negatively (left)- and positively (right)-oriented line solitons (referred in what follows as r-solitons and l-solitons). At "time" y, $f^{\alpha}(a;x,y)\mathrm{d}a\mathrm{d}x$ represents the number of α solitons (α being either l or r) in the element $[a, a+\mathrm{d}a] \times [x, x+\mathrm{d}x]$ of the phase space $A^{\alpha} \times \mathbb{R}$, A^{α} being the "spectral support" of the respective DOS under conventional SG terminology [17]. We should stress that the (x, y) variations of the total DOS, $f(a;x,y) = f^{\mathrm{l}}(a;x,y) + f^{\mathrm{r}}(a;x,y)$, in a nonhomogeneous SG, occur on a hydrodynamic scale much larger than the "mesoscopic" scale where the gas is locally homogeneous, itself much larger than the microscopic scale of variations of the wave field (the coherence length), see [18].

The collision rate ansatz of [5] applied to the Boussinesq equation yields the stationary projection of the kinetic equation for the weakly nonuniform KPII SG in the form of two continuity equations describing the DOS's spatial variations in (x, y) plane,

$$f^{\mathrm{l}}_y + (s^{\mathrm{l}} f^{\mathrm{l}})_x = 0, \quad f^{\mathrm{r}}_y + (s^{\mathrm{r}} f^{\mathrm{r}})_x = 0, \tag{5}$$

where $s^{\mathrm{l,r}}(a;x,y)$ are the effective slope parameters satisfying the coupled integral equations of state, dropping the (x, y) dependence for brevity

$$s^{\alpha}(a) = c^{\alpha}(a) + \sum_{\gamma=\alpha,\beta} \int_{A^{\gamma}} \Delta(a,a') f^{\gamma}(a')[s^{\alpha}(a) - s^{\gamma}(a')]\mathrm{d}a', \tag{6}$$

where $\Delta(a, a') = \varphi(a, a')/a$ is the position shift, α is either l ($c^{l}(a) = -\sqrt{1-4a^2}$) or r ($c^{\mathrm{r}}(a) = \sqrt{1-4a^2}$), β is either r or l respectively. The equations of state (6) are consistent with the Euler GHD of the Boussinesq SG constructed in [24].

As an illustration, and to highlight some salient features of the stationary KPII SGs, we will now discuss a paradigmatic example for which we can extract exact analytic results. Following [3,5,54,55] we introduce the "polychromatic" delta-functional ansatz for both species' DOS,

$$\begin{aligned} f^{\mathrm{r}}(a;x,y) &= \sum_{i=1}^{M^{\mathrm{r}}} F^{\mathrm{r}}_i(x,y)\delta\big(a - a^{\mathrm{r}}{}_i\big), \\ f^{\mathrm{l}}(a;x,y) &= \sum_{i=M^{\mathrm{r}}+1}^{M^{\mathrm{r}}+M^{\mathrm{l}}} F^{\mathrm{l}}_i(x,y)\delta\big(a - a^{\mathrm{l}}_i\big), \end{aligned} \tag{7}$$

where $M^{\mathrm{l,r}}$ are the numbers of components of the respective soliton species. As a matter of fact, this polychromatic reduction is an idealisation and, in practice, amplitudes are considered to be uniformly distributed around a^{α}_i in small intervals of size ϵ_g. Substituting (7) in the kinetic equations (5) and (6) yields a system of hydrodynamic conservation laws for $F^{\mathrm{l}}_i(x,y)$ and $F^{\mathrm{r}}_i(x,y)$,

$$\big(F^{\mathrm{r}}_i\big)_y + \big(s^{\mathrm{r}}_i F^{\mathrm{r}}_i\big)_x = 0, \quad \big(F^{\mathrm{l}}_j\big)_y + \big(s^{\mathrm{l}}_j F^{\mathrm{l}}_j\big)_x = 0, \tag{8}$$

$i = 1,\dots M^{\mathrm{r}}$, $j = M^{\mathrm{r}}+1,\dots,M^{\mathrm{r}}+M^{\mathrm{l}}$, complemented by a system of algebraic closure equations connecting the components' slope parameters $s^{\mathrm{l}}_i \equiv s^{\mathrm{l}}(a^{\mathrm{l}}_i)$, $s^{\mathrm{r}}_i \equiv s^{\mathrm{r}}(a^{\mathrm{r}}{}_i)$ with the densities F^{l}_i, F^{r}_i. In particular, for the two-component, "bichromatic", SG $(M^{\mathrm{l}} + M^{\mathrm{r}} = 2)$ we have explicit expressions,

$$s^{\alpha}_1 = c^{\alpha}_1 + \frac{\big[c^{\alpha}_1 - c^{\beta}_2\big]\Delta_{12}F^{\beta}_2}{1 - \big[\Delta_{12}F^{\beta}_2 + \Delta_{21}F^{\alpha}_1\big]}, \tag{9a}$$

$$s^{\beta}_2 = c^{\beta}_2 - \frac{\big[c^{\alpha}_1 - c^{\beta}_2\big]\Delta_{21}F^{\alpha}_1}{1 - \big[\Delta_{12}F^{\beta}_2 + \Delta_{21}F^{\alpha}_1\big]}. \tag{9b}$$

It is important to stress that the bichromatic reductions are subject to the constraint $1 - (\Delta_{12}F^{\beta}_2 + \Delta_{21}F^{\alpha}_1) > 0$, which implies that the denominators in (9) must be positive [55].

The hydrodynamic reductions of the kinetic equation were shown in [54] to be linearly degenerate integrable systems of hydrodynamic type, which implies the absence of wave breaking and the admissibility of contact discontinuities in solutions of canonical Riemann problems [3,5,55].

IV. LINE SOLITON REFRACTION AND OBLIQUE INTERFERENCE OF SGs

We consider bichromatic SGs to describe the following prototypical interaction problems: (i) 2D refraction of a line soliton by a one-component (monochromatic) SG; (ii) oblique interference of two monochromatic SGs. Each of these problems includes two qualitatively different configurations: (a) codirectional refraction/interference when both the trial soliton and the SG in Problem (i) or two monochromatic SGs in Problem (ii) have the same orientation; and (b) counterdirectional refraction/interference when the trial soliton and the SG or two interacting SGs have opposite orientations. We shall use the shorthand notation "r-r" for the two-component interaction with both gas components having right orientation and "r-l" if the 1st component has right orientation and the second-left orientation etc. Moreover, in the context of the polychromatic reduction we shall use the notation $c^{\alpha}_i \equiv c^{\alpha}(a^{\alpha}_i)$.

A. Line soliton refraction by a SG

The interaction of a single soliton with macroscopic dispersive hydrodynamic structures such as rarefaction and dispersive shock waves in 1D has been the subject of active recent research, see [56–62]. This purely deterministic setting was extended to the case of the interaction of a soliton with a random wave field in [15], where the "temporal" isotropic refraction of an optical soliton interacting with a dense 1D SG

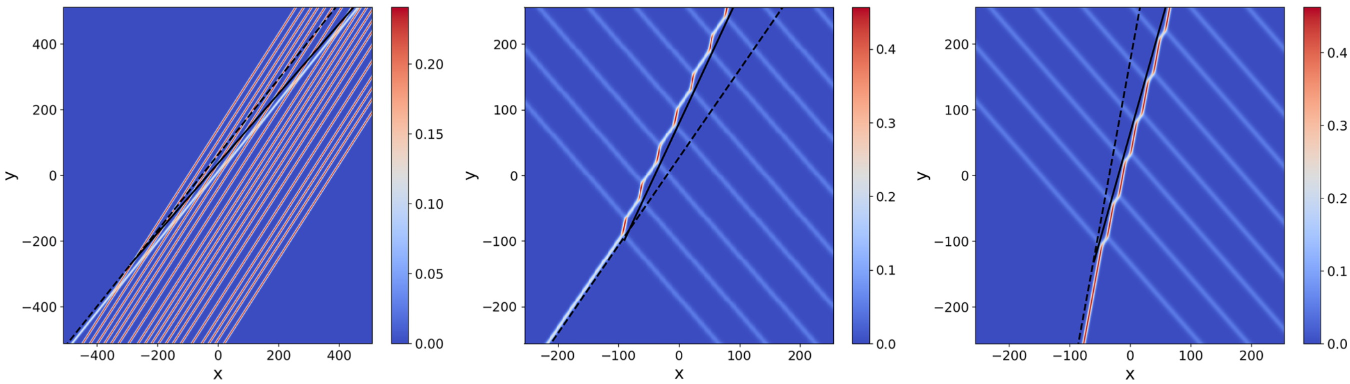

FIG. 1. Refraction of a trial line soliton by a monochromatic 2D stationary KPII SG composed of $N_g = 19$ solitons. (Left) Codirectional, r-r refraction of a trial soliton with spectral (amplitude) parameter $a^{\rm r}{}_1 = 0.25$ by a monochromatic 2D stationary SG with spectral parameter $a^{\rm r}{}_2 = 0.366$, density $F_2^{\rm r} = 0.04$, and the "physical" spectral width of the monochromatic component $\epsilon_g = 1 \times 10^{-3}$. (Center and right) Counterdirectional, r-l refraction of a trial line soliton by a monochromatic 2D stationary SG with spectral parameter $a_2^{\rm l} = 0.158$, density $F_2^{\rm l} = 0.013$, and $\epsilon_g = 1 \times 10^{-6}$. The spectral parameters of the trial soliton are $a^{\rm r}{}_1 = 0.49$ (middle panel, negative refraction) and $a^{\rm r}{}_1 = 0.3318$ (right panel, positive refraction). The black-dashed lines represent the slope of a noninteracting line soliton, and the black-solid lines represent the analytically predicted effective slope of the trial r-soliton resulting from the cumulative phase shift in the interaction with the SG.

in an optical fiber has been observed in a laboratory experiment, and the observed refraction parameters were favorably compared with the analytical predictions of the SG kinetic theory for the focusing NLS equation [4].

Here, we study the soliton refraction phenomenon in its original, spatial, context by considering the interaction of a KPII line soliton with a stationary 2D SG. We use the polychromatic reduction of the kinetic equation as a convenient mathematical framework where exact analytical results are available, and which, at the same time, reveals the basic phenomenology of the 2D SG refraction.

(a) *Codirectional r-r refraction*. (The l-l case is analogous). In this case $M^{\rm r} = 2$, $M^{\rm l} = 0$ in the hydrodynamic system (8), and we use the bi-chromatic reduction (9) of the equation of state with $\alpha = \beta = r$. To describe the refraction of a single r-soliton of amplitude $a^{\rm r}{}_1$ by the right-oriented monochromatic SG with the amplitude $a^{\rm r}{}_2 > a^{\rm r}{}_1$, slope parameter $c_2^{\rm r} < c_1^{\rm r}$, and density $F_2^{\rm r}$, we further set $F_1^{\rm r} = 0$ in (9) so that the effective slope parameter of the refracted soliton is given by

$$s_1^{\rm r} = c_1^{\rm r} + \frac{\left[c_1^{\rm r} - c_2^{\rm r}\right]\Delta^{\rm co}\left(a_1^{\rm r}, a_2^{\rm r}\right)F_2^{\rm r}}{1 - \Delta^{\rm co}\left(a_1^{\rm r}, a_2^{\rm r}\right)F_2^{\rm r}}, \tag{10}$$

whereas for the SG we have $s_2^{\rm r} = c_2^{\rm r}$ (a single trial soliton does not significantly alter the slope of the SG). Since $\Delta^{\rm co} < 0$, it follows from (10) that $\mathrm{sgn}[s_1^{\rm r} - c_1^{\rm r}] = -1$, i.e., the codirectional refraction is always positive, according to the conventional ray optics terminology. See Fig. 1(left) for a typical codirectional refraction configuration.

(b) *Counterdirectional r-l refraction*. We set $M^{\rm r} = M^{\rm l} = 1$, $\alpha = r$, $\beta = l$ so that the equations of state (9) yield, upon further setting $F_1^{\rm r} = 0$, the effective slope parameter for the refracted r-soliton,

$$s_1^{\rm r} = c_1^{\rm r} + \frac{\left[c_1^{\rm r} - c_2^{\rm l}\right]\Delta^{\rm ct}\left(a_1^{\rm r}, a_2^{\rm l}\right)F_2^{\rm l}}{1 - \Delta^{\rm ct}\left(a_1^{\rm r}, a_2^{\rm l}\right)F_2^{\rm l}}, \tag{11}$$

whereas the SG slope parameter is $s_2^{\rm l} = c_2^{\rm l}$. Since $(1 - \Delta^{\rm ct}(a^{\rm r}{}_1, a_2^{\rm l})F_2^{\rm l}) > 0$, $\mathrm{sgn}[s_1^{\rm r} - c_1^{\rm r}] = \mathrm{sgn}\,(\Delta^{\rm ct}(a^{\rm r}{}_1, a_2^{\rm l})[c_1^{\rm r} - c_2^{\rm l}])$ can be either positive or negative. See Fig. 1 for the numerical demonstration of the negative (middle panel) and positive (right panel) counterdirectional 2D soliton refraction.

Comparison of the analytically determined effective refraction slope parameters (10), (11) with the results of direct numerical implementation of the 2D line soliton refraction problems for KPII, in Fig. 2, demonstrates excellent agreement. See Sec. VI and Appendix C for details of the numerical simulations.

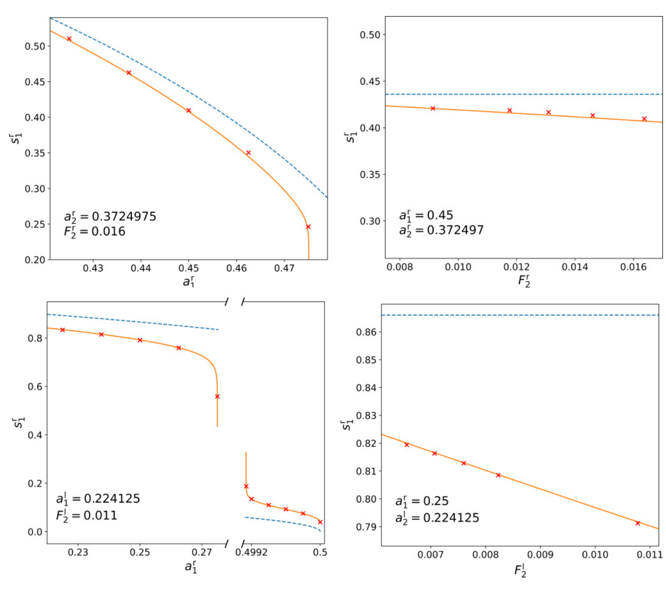

FIG. 2. Effective slope $s_1^{\rm r}$ for the codirectional (top) and counterdirectional (bottom) refraction of a soliton of amplitude $a^{\rm r}{}_1$ by a monochromatic SG with the amplitude and density parameters a_2^α and F_2^α, respectively. The SG is composed of $N = 100$ solitons with the spectral (amplitude) parameters distributed over the narrow interval of width $\epsilon_g = 2.5 \times 10^{-9}$, see Sec. VI and Appendix C for details of the numerical implementation of SGs. Shown is the comparison between the theoretical prediction (solid line) and numerics (red cross). The dashed-blue curves show the slope parameter of a noninteracting trial line soliton.

B. Oblique interference of two monochromatic SGs

The *oblique interference* of two monochromatic line SGs is described by the solution of the Riemann problem for the hydrodynamic system (8), (9) with $M^l + M^r = 2$, specifying a one-component density at each side of $x = 0$ at $y = 0$,

$$F_1^\alpha(x,0) = F_{10}^\alpha,\ F_2^\beta(x,0) = 0 \ \text{ if } x < 0, \tag{12}$$

$$F_1^\alpha(x,0) = 0,\ F_2^\beta(x,0) = F_{20}^\beta \ \text{ if } x > 0. \tag{13}$$

The dependence of the "initial" velocities $s_1^\alpha(x,0)$, $s_2^\beta(x,0)$ on the densities $F_1^\alpha(x,0)$, $F_2^\beta(x,0)$ is defined by the relations (9). Owing to the scale invariance of the Riemann problem, the solution is a self-similar distribution $F_1^\alpha(x/y)$, $F_2^\beta(x/y)$. Because of linear degeneracy of the hydrodynamic system [(8) and (9)], see [54], the only admissible similarity solutions are constant states separated by propagating contact discontinuities, see for instance [63]. Discontinuous weak solutions are physically admissible here since the kinetic equation describes the conservation of the number of solitons within any given spectral interval, and the Rankine-Hugoniot type conditions can be imposed to ensure the conservation of the number of solitons across the discontinuities. As a result, the solution of the Riemann problem [(8) and (14)] for each component is composed of three constant states separated by two contact discontinuities [3,17,64],

$$\left(F_1^\alpha(x,y), F_2^\beta(x,y)\right) = \begin{cases} (F_{10}^\alpha, 0), & x/y < c^-, \\ \left(F_{1c}^\alpha, F_{2c}^\beta\right), & c^- < x/y < c^+, \\ \left(0, F_{20}^\beta\right), & x/y > c^+, \end{cases} \tag{14}$$

where the component densities F_{1c}^α and F_{2c}^β in the interference region $c^- y < x < c^+ y$ and the inverse slopes of the contact discontinuities $c^\pm$ are found for the Rankine-Hugoniot conditions $-c[\![F_i^\gamma]\!] + [\![F_i^\gamma s_i^\gamma]\!] = 0$, $i = 1, 2$ applied across $x = cy$. Here, c is either c^- (left discontinuity) or c^+ (right discontinuity) and $[\![F]\!]$ denotes the jump of F across the discontinuity. As a result one obtains

$$c^+ = c_1^\alpha + \frac{\left[c_1^\alpha - c_2^\beta\right]\Delta_{1,2}F_{20}^\beta}{1 - \Delta_{2,1}F_{20}^\beta}, \tag{15a}$$

$$c^- = c_2^\beta - \frac{\left[c_1^\alpha - c_2^\beta\right]\Delta_{2,1}F_{10}^\alpha}{1 - \Delta_{1,2}F_{10}^\alpha}. \tag{15b}$$

The component densities in the interference region are given by

$$F_{1c}^\alpha = \frac{F_{10}^\alpha\left[1 - \Delta_{1,2}F_{20}^\beta\right]}{1 - \Delta_{1,2}\Delta_{2,1}F_{10}^\alpha F_{20}^\beta}, \tag{16a}$$

$$F_{2c}^\beta = \frac{F_{20}^\beta\left[1 - \Delta_{2,1}F_{10}^\alpha\right]}{1 - \Delta_{1,2}\Delta_{2,1}F_{10}^\alpha F_{20}^\beta}, \tag{16b}$$

where $\Delta_{i,j} = \Delta(a_i^\alpha, a_j^\beta)$. For codirectional r-r oblique interference, $\alpha = \beta = r$; for r-l interference, $\alpha = r$, $\beta = l$. As one can see, the leading contact discontinuity slope (15a) coincides with the refraction slope of a single-line soliton for codirectional (10) and for counterdirectional (11) interference.

The two prototypical oblique nonlinear interference configurations are illustrated in Fig. 3; the positions of the contact discontinuities defined by (15a) and (15b) are shown in black-solid lines and display excellent agreement with numerical results. One can see that nonlinear soliton interaction widens the interference region, while in the counterdirectional case the effect is opposite, consistent with the signs of the respective two-soliton phase shifts (4). One can also observe the qualitative difference in the geometry of the interference patterns with the characteristic "honeycomb SG" signature in the counter-directional case. The spatial distribution of the KPII wave field in the stationary honeycomb SG is illustrated in Fig. 4.

V. CORRELATIONS

We now consider the spatial correlations for the 2D bichromatic SGs. These can be evaluated by mapping the GHD results for Boussinesq SGs [24,65], to the $(2+0)$D KPII setup. We refer the interested reader to these two references for a more in depths discussion.

We first need to define a quantity that is fundamental in GHD: the occupation function. Like the DOS, it comes in two flavours, the *left* and *right occupation*, n^{l} and n^{r}, defined by

$$\frac{2\pi f^\alpha(a)}{n^\alpha(a)} = a + \sum_{\gamma=\alpha,\beta}\int_{A^\gamma} \mathrm{d}a' f^\gamma(a')\Delta(a,a'), \tag{17}$$

where, as earlier, α is either l or r, and β is r or l respectively. This quantity is used to define the left- and right-dressing operations

$$g^{\alpha,\mathrm{dr}}(a) = g(a) + \sum_{\gamma=\alpha,\beta}\int_{A^\gamma}\frac{\mathrm{d}a'}{2\pi}\Delta(a,a')n^\gamma(a')g^{\gamma,\mathrm{dr}}(a'), \tag{18}$$

for any smooth function $g(a)$. The horizontal covariance of the wave field is then given as [24]

$$\int_{\mathbb{R}} \mathrm{d}x\langle u(x,y)u(0,y)\rangle^c = \sum_{\gamma=\alpha,\beta}\int_{A^\gamma}\mathrm{d}a f^\gamma(a;0,y)\left(h_0^{\gamma,\mathrm{dr}}(a;0,y)\right)^2, \tag{19}$$

where $h_0(a) = 4a$. This particularly simple form of $h_0(a)$ comes from the fact that the wave field u is also the density of the first conserved quantity associated with the Boussinesq equation $Q_0 = \int \mathrm{d}x\, u(x,y)$, $\partial_y Q_0 = 0$, and $h_0(a) \equiv 4a$ corresponds to Q_0 evaluated for a single-soliton solution of amplitude a {cf. [24] for details and Appendix B for the evaluation of the dressing of $h_0(a)$}.

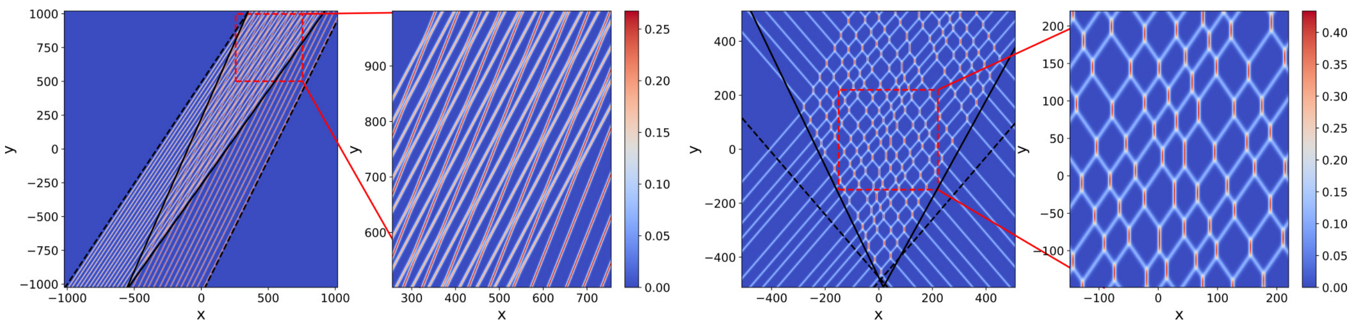

FIG. 3. Oblique nonlinear interference of two stationary monochromatic SGs for the KPII equation. (Left) Codirectional interference. SG parameters: $a_1^{\mathrm{r}} = 0.3715$, $F_1^{\mathrm{r}} = 0.036$, $a_2^{\mathrm{r}} = 0.433012$, $F_2^{\mathrm{r}} = 0.028$, $N_1^{\mathrm{r}} = N_2^{\mathrm{r}} = 15$, and $\epsilon_g = 1.0 \times 10^{-4}$. (Right) Counterdirectional interference. SG parameters: $a_1^{\mathrm{r}} = 0.25$, $F_1^{\mathrm{r}} = 0.017$, $a_2^{\mathrm{l}} = 0.25$, $F_2^{\mathrm{l}} = 0.014$, $N_1^{\mathrm{r}} = N_1^{\mathrm{l}} = 15$, and $\epsilon_g = 1.0 \times 10^{-4}$. The dashed lines show the slopes of the monochromatic SGs outside the interaction region; the black-solid lines delimit the boundaries of the nonlinear interference region defined by the slopes of hydrodynamic contact discontinuities given by (15).

One can also evaluate two-point correlations as

$$\begin{aligned} &\frac{1}{2L}\int_{-L}^{L} \mathrm{d}x' \langle u(x+x', y)u(0,0)\rangle^c \\ &\quad = \sum_{\gamma=\alpha,\beta} \int_{A^\gamma} \mathrm{d}a\, \delta(x - s^\gamma(a;0,0)y) f^\gamma(a;x,y) \\ &\quad\quad \times h_0^{\gamma,\mathrm{dr}}(a;x,y) h_0^{\gamma,\mathrm{dr}}(a;0,0) \\ &\quad \sim \frac{1}{y} \sum_{\gamma=\alpha,\beta} \sum_{a\in a_*^\gamma} \frac{f^\gamma(a;0,0)}{|\partial_a s^\gamma(a;0,0)|} \big(h_0^{\gamma,\mathrm{dr}}(a;0,0)\big)^2, \end{aligned} \tag{20}$$

for $y \gg L \gg \ell$, where $\ell = [\sum_{\gamma=\alpha,\beta} \int_{A^\gamma} \mathrm{d}a f^\gamma(a;0,0)]^{-1}$ quantifies the average intersoliton spacing along the x direction, and $a_*^\gamma = \{a : s^\gamma(a;0,0) = x/y\}$.

We now apply general results [(19) and (20)] to the case of bichromatic SGs. Within any region of (x, y) where the SG is statistically homogeneous (e.g., in the honeycomb SG region in the right panel of Fig. 3, see also Fig. 4), we have from (19) (see Appendix B)

$$\int_{\mathbb{R}} \mathrm{d}x\, \langle u(x,y)u(0,0)\rangle^c = 16\big[\big(a_2^\beta\big)^2 F_1^\alpha + \big(a_1^\alpha\big)^2 F_2^\beta\big], \tag{21}$$

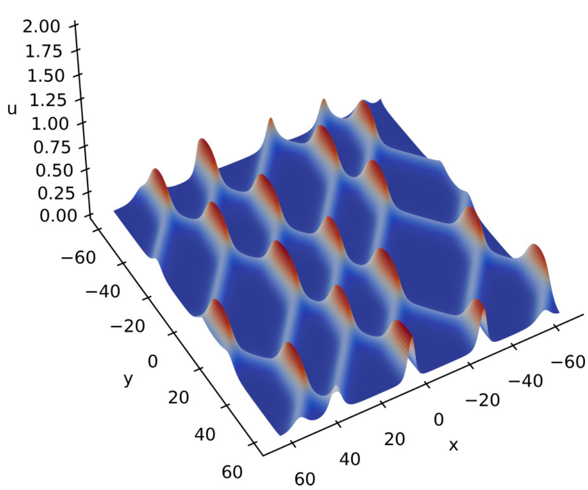

FIG. 4. Spatial distribution of the wave field $u(x, y)$ in the KPII stationary honeycomb soliton gas.

(α, β) being defined as in Eqs. (15), and $\langle u(x,y)u(0,0)\rangle^c = \langle u(x,y)u(0,0)\rangle - \langle u(x,y)\rangle\langle u(0,0)\rangle$ being the connected correlation. Note that the right-hand side does not depend on y, because the field u is a conserved density of the Boussinesq equation.

Nontrivial two-point correlations in a polychromatic gas arise owing to the inevitably present physical spectral broadening $\sim\epsilon_g$ around the points a_i^α in the DOS (7). This becomes significant because two-point correlations have to be evaluated over sufficiently large scales, on which the gas cannot be considered homogeneous anymore. Over such large scales, the slight difference between the spectral parameter of a given soliton within the gas and the reference value a_i^α may translate, through the multiple scattering shifts it incurs, into a meaningful deviation from its reference trajectory $s^\gamma(a_i^\alpha) = x/y$. As such, we can define a "light cone" by computing the effective velocities $s_{i,-}^\gamma$ and $s_{i,+}^\gamma$ a soliton of amplitude $a_{i,-}^\alpha = a_i^\alpha - \epsilon_g/2$ and one of amplitude $a_{i,+}^\alpha = a_i^\alpha + \epsilon_g/2$ would have if they interacted with the polychromatic gas (see Appendix B for details).

Then along a given effective slope direction (e.g., s_1^α) we obtain

$$\frac{1}{2L}\int_{-L}^{L} \mathrm{d}x \langle u(s_1^\alpha Y + x, Y)u(0,0)\rangle^c \sim \frac{16\big(a_2^\beta\big)^2 F_1^\alpha}{Y\epsilon_g\big|\partial_{a_1^\alpha} s_1^\alpha\big|} \tag{22}$$

for $L \gg \max[\delta(Y, \epsilon_g), \ell]$, and $Y \gg L$. Here, $\ell = [F_1^\alpha + F_2^\beta]^{-1}$ quantifies the average intersoliton spacing along the x direction, and $\delta(Y, \epsilon_g)$ is the size of the interval around $x = s_1^\alpha Y$ at which the soliton would intersect with the horizontal, given ϵ_g, at $y = Y$ (the result should be independent of the precise choice of L). Note that for a fixed $\epsilon_g > 0$ these correlations exhibit the $1/y$ ballistic scaling typical of many-body integrable systems [21].

VI. NUMERICAL IMPLEMENTATION OF 2D SOLITON GAS

The numerical implementation of 2D SGs studied in this paper is achieved via exact multisoliton solutions of the full Galilean-boosted KPII equation configured accordingly to the designed DOS. The numerical algorithm relies on the Wronskian formulation of the N-soliton solution, and

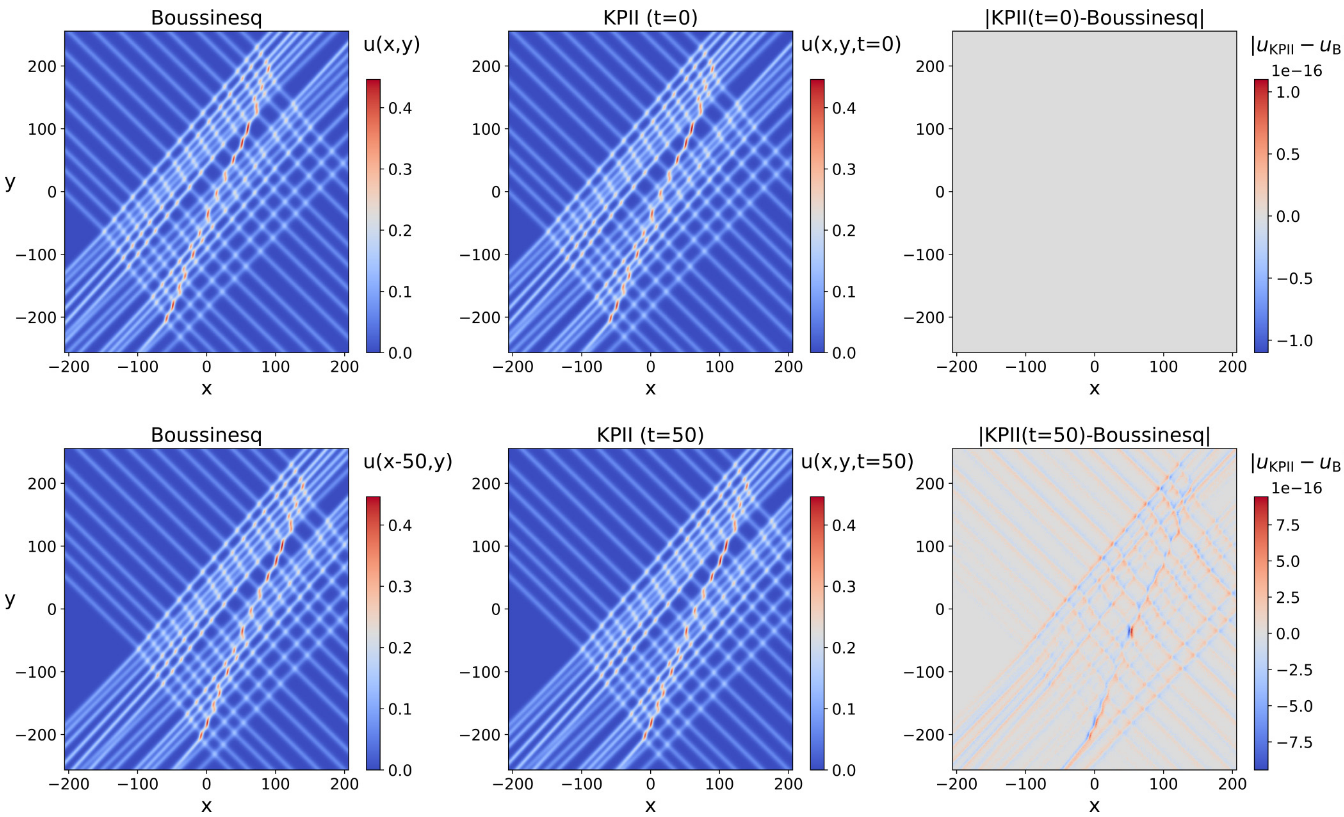

FIG. 5. Comparison of 2D line SG interference implemented via exact N-soliton solution of the Boussinesq (left) and KPII (centre) equations and the absolute value of the difference between the solutions generated using the two different algorithms (right). The positively sloped gas is composed of $N^{\mathrm{r}} = 15$ solitons with parameter a^{r} uniformly distributed in the range $a^{\mathrm{r}} \in [0.175, 0.281]$. The negatively sloped gas is composed of $N^{\mathrm{l}} = 15$ solitons with parameter a^{l} uniformly distributed in the range $a^{\mathrm{l}} \in [0.175, 0.183]$. (Top row) KPII solution generated at $t = 0$ compared with the Boussinesq solution. Note that the difference is identical to zero up to the accuracy used to save the data. (Bottom row) KPII solution generated at $t = 50$ compared with the Boussinesq solution shifted by $\Delta x = 50$, according to the Galilean-boost adopted. Note that the difference is of the order of magnitude of the accuracy used to save the data.

high-precision arithmetic routines are included to overcome the numerical accuracy problems arising for $N \gg 1$. See Appendix C for details of the numerical implementation of N-soliton KP solutions.

The monochromatic SGs are approximated by N-soliton solutions consisting of a "cluster" of N solitons with parameters a_i uniformly distributed in a small region of width ϵ_g centered at a_g. Additionally, the randomness of the soliton ensemble approximating the SG is realized by generating soliton phases x_{0j} as independent random values uniformly distributed on some interval of width δ_x, which determines the spatial density F_g of the gas. The latter is computed numerically as the ratio between the selected number of solitons N in the gas over its spatial extent L in the x direction: $F_g = N/L$. See [55,66] for the description of the relation between δ_x and F_g for the KdV SG.

In parallel with KPII SG computations we performed numerical synthesis of the Boussinesq SG using a different algorithm (see Appendix C). At $t = 0$ both solutions are identical. We then compare the KPII SG at $t = 50$ with the Boussinesq SG solution shifted by $\Delta x = 50$ to compensate for the Galilean boost adopted in the KPII. The comparison shows that the difference between the two solutions is within the numerical accuracy associated with data saving, confirming the robustness of our numerical algorithms (see Fig. 5 in Appendix C).

VII. DISCUSSION

Summarizing, we have constructed spectral theory of 2D stationary SGs for the KPII equation. This has been done using the steady-state reduction of the KPII equation to the (1+1) integrable two-way Boussinesq equation and applying the recently developed kinetic theory of bidirectional SGs [5] and the GHD of the Boussinesq equation [24]. Using the polychromatic, delta-function reductions of the spectral kinetic equation for the Boussinesq equation we have considered two basic 2D SG interaction problems: (i) refraction of a line soliton by a spectrally "monochromatic" SG; and (ii) oblique interference of two SGs described by weak solution of the stationary Riemann problem. Analytical predictions regarding the 2D SG interactions are shown to be in excellent agreement with the direct numerical implementation of 2D stationary SGs using appropriately configured exact N-soliton solutions of the KPII equation. We have also computed the spatial correlations in the polychromatic 2D SGs by mapping the GHD results for Boussinesq SGs [24], to the (2+0)D KPII setup.

The phenomena of 2D soliton refraction and SG interference can be potentially realised in a 2D shallow water tank, e.g., using the setting similar to [9]. The oblique SG interference can also be used for the modeling of the crossing sea type phenomena in the ocean [67].

Our results represent the first step in the development of the kinetic theory of 2D SGs. A natural next step will be the formulation of an analytical description of nonstationary SGs of the full KPII equation, which will include a variety of physical phenomena such as soliton resonance and web structure [38–42] not accounted for in the stationary reduction.

ACKNOWLEDGMENTS

The authors thank the Isaac Newton Institute for Mathematical Sciences, Cambridge, for support and hospitality during the programme "Emergent phenomena in nonlinear dispersive waves", where work on this paper was undertaken. This work was supported by Engineering and Physical Sciences Research Council (EPSRC) Grant No. EP/R014604/1. T.B. and B.D. were further supported by the EPSRC under Grant No. EP/W010194/1. The work of G.A.E. and G.R. was also supported by the EPSRC Grant No. EP/W032759/1. The authors thank R. Dubertrand for sharing C. Schmit's algorithm for efficiently computing matrix determinants.

DATA AVAILABILITY

No data were created or analyzed in this article.

APPENDIX

1. Multisoliton solutions

It is easy to see that the Galilean-boosted KPII equation, i.e., the PDE

$$(u_t - u_x + 6uu_x + u_{xxx})_x + u_{yy} = 0, \tag{A1}$$

can be obtained from the standard KPII equation via the change of independent variables $x' = x - t$, $y' = y$, and $t' = t$. Accordingly, Eq. (A1) admits a large class of solutions expressed via the Wronskian formalism [39,42,50,51]:

$$u(x, y, t) = 2\frac{\partial^2}{\partial x^2}\log\tau(x, y, t), \tag{A2}$$

where the "tau" function $\tau(x, y, t)$ satisfies Hirota's bilinear equation [51]. It was then shown in [50] that solutions of Hirota's bilinear equation can be obtained in terms of Wronskians,

$$\tau(x, y, t) = \mathrm{Wr}(f_1, \dots, f_N) = \det\begin{pmatrix} f_1 & f_2 & \cdots & f_N \\ f_1^{(1)} & f_2^{(1)} & \cdots & f_N^{(1)} \\ \vdots & \vdots & \ddots & \vdots \\ f_1^{(N-1)} & f_2^{(N-1)} & \cdots & f_N^{(N-1)} \end{pmatrix}, \tag{A3}$$

where $f_n\o j = \partial^j f/\partial x^j$, and $f_1, \dots, f_N$ satisfy the linear PDEs

$$\frac{\partial f_n}{\partial y} = \sqrt{3}\,\frac{\partial^2 f_n}{\partial x^2}, \quad \frac{\partial f_n}{\partial t} = \frac{\partial f_n}{\partial x} - 4\frac{\partial^3 f_n}{\partial x^3}. \tag{A4}$$

Multisoliton solutions of (A1) are obtained by choosing $f_1, \dots, f_N$ as linear combinations of exponentials,

$$f_n(x, y, t) = \sum_{m=1}^{M} g_{n,m}\mathrm{e}^{\theta_m}, \tag{A5}$$

where, similarly to [39], the exponential "phases" $\theta_1, \dots, \theta_M$ are given by

$$\theta_m = k_m x + \sqrt{3}k_m^2 y + \big(k_m - 4k_m^3\big)t + \theta_{m,0}. \tag{A6}$$

The above solution is uniquely determined by the "phase parameters" $k_1, \dots, k_M$ and the $N \times M$ coefficient matrix $G = (g_{n,m})$, plus the "translation constants" $\theta_{1,0}, \dots, \theta_{M,0}$. Without loss of generality, one can take the phase parameters to be ordered so that $k_1 < \cdots < k_M$.

The simplest nontrivial case is obtained when $N = 1$ and $M = 2$. In this case, one recovers the soliton solution (3) of the KPII equation. It is convenient to label the two phase parameters as k_- and k_+ in this case. The corresponding amplitude and slope parameters a and c are then given by the map

$$a = \tfrac{1}{2}(k_+ - k_-), \quad c = -\sqrt{3}\,(k_+ + k_-), \tag{A7a}$$

which is inverted by

$$k_\pm = \pm a - c/(2\sqrt{3}). \tag{A7b}$$

For the Boussinesq equation [Eq. (2) of the main text], since a is fixed by the dispersion relation

$$c = \pm\sqrt{1 - 4a^2}, \tag{A8}$$

$k_\pm$ can instead be expressed in terms of the single parameter c as

$$k_\pm = \tfrac{1}{2}(\pm\sqrt{1 - c^2} - c/\sqrt{3}). \tag{A9}$$

For arbitrary values of N and M, the Wronskian representation (A3) with $f_1, \dots, f_N$ as in (A5) yields

$$\tau(x, y, t) = \det(K\,\mathrm{e}^{\Theta}G^T) = \sum_{1\leqslant m_1 < m_2 < \cdots < m_N \leqslant M} V_{m_1,\dots,m_N}\, G_{m_1,\dots,m_N}\, \mathrm{e}^{\theta_{m_1}+\cdots+\theta_{m_N}}, \tag{A10}$$

where $\Theta = \mathrm{diag}(\theta_1, \dots, \theta_M)$, the $N \times M$ matrix K is given by $K = (k_m^{n-1})$, $V_{m_1,\dots,m_N} > 0$ is a Van der Monde determinant, and $G_{m_1,\dots,m_N}$ is the determinant of the $N \times N$ minor obtained from columns $m_1, \dots, m_N$ of G. Note that the spatiotemporal dependence of the tau function is confined to the exponential phases.

For irreducible coefficient matrices, the above representation produces a solution with exactly N asymptotic line solitons as $y \to \infty$ and $M - N$ asymptotic line solitons as $y \to -\infty$ [39]. The amplitude and slope of each asymptotic line soliton are completely determined by a pair of phase parameters among $k_1, \dots, k_M$, but the precise pair associated to each soliton depends on the choice of coefficient matrix

G. Importantly, in order for solutions to be nonsingular, all the $N \times N$ minors of the associated coefficient matrix G are non-negative.

A Wronskian formulation for the multisoliton solutions of the Boussinesq equation was given in [68], but it can be immediately obtained as a reduction of the above formalism for the KPII equation, except that one has additional restrictions on the choice of phase parameters, as we discuss next. Specifically, suppose that one wants to construct a multisoliton solution consisting of two line solitons with amplitude and slope parameters (a_1, c_1) and (a_2, c_2). One obviously needs $N = 2$ and $M = 4$. Denote the two sets of phase parameters, one set associated to each soliton, as $k_{1,\pm}$ and $k_{2,\pm}$, respectively. The resulting two-soliton solution differs depending on the relative ordering of $k_{2,\pm}$ compared to $k_{1,\pm}$ [41]. Further, each of the above three cases corresponds to a different kind of soliton interaction [40]. Specifically, and taking $k_{1,-} < k_{2,-}$ without loss of generality, there are three different classes of solutions, corresponding to the following three possible cases:

(i) Ordinary soliton interaction: $k_{1,+} < k_{2,-}$ (corresponding to no overlap between $k_{1,\pm}$ and $k_{2,\pm}$), which occurs if and only if

$$(c_2 - c_1)/(2\sqrt{3}) + a_1 + a_2 < 0. \tag{A11a}$$

This corresponds to "standard" soliton interactions: The two solitons emerge unscathed after their interaction, except for a positive phase shift.

(ii) Resonant soliton interaction: $k_{2,-} < k_{1,+} < k_{2,+}$ (corresponding to partial overlap between $k_{1,\pm}$ and $k_{2,\pm}$), which occurs if and only if

$$-(a_1 + a_2) < (c_2 - c_1)/(2\sqrt{3}) < a_2 - a_1. \tag{A11b}$$

Resonant two-soliton interactions produce a complex, time-dependent box-shaped pattern [38], in which, at each vertex, two solitons merge into one, producing a local Y shape characterized by a so-called Miles soliton resonance [69,70].

(iii) Asymmetric soliton interaction: $k_{1,+} > k_{2,+}$ (corresponding to "total overlap" between $k_{1,\pm}$ and $k_{2,\pm}$), which occurs if and only if

$$c_2 - c_1 > 2\sqrt{3}\,(a_1 + a_2). \tag{A11c}$$

Asymmetric interactions are similar to ordinary ones, the only difference being that solitons incur a negative phase shift.

The inequalities (A11) cover the whole soliton parameter space (a_1, a_2, c_1, c_2) for the KPII equation. On the other hand, the above trichotomy has important consequences in terms of the reduction to the Boussinesq equation, since only ordinary and asymmetric pairwise two-soliton interactions lead to stationary solutions. One must, therefore, impose a pairwise nonresonance condition on the parameters of the individual solitons. That is, one must impose that each pair of phase parameters has either no overlap or total overlap with every other pair. Moreover, when the relation (A8) is taken into account, (A11) imposes additional restrictions on the allowable choices of slopes, with the result that not all possible pairs c_1 and c_2 are admissible. This phenomenon was first pointed out in [53] and put in the context of the KP formalism in [52], where an alternative formulation of the multisoliton solutions of the Boussinesq equation was given, and it was shown that N-soliton solutions of Eq. (2) can be expressed via Eq. (A2), where now the tau function is the determinant of an $N \times N$ matrix, namely,

$$\tau(x, y, t = 0) = \det(I + M), \tag{A12}$$

where I is the $N \times N$ identity matrix and $M = (M_{jk})$, with

$$M_{jk} = \frac{C_j}{\mu_j - \lambda_k} \exp\left[\frac{\mu_j - \lambda_j}{2}\left(x - \frac{\sqrt{3}}{2}(\mu_j + \lambda_j)y\right)\right], \tag{A13}$$

and where the real-valued parameters μ_j and λ_j are related by the constraint

$$2\mu_j + \lambda_j \pm \sqrt{4 - 3\lambda_j^2} = 0. \tag{A14}$$

By computing the one-soliton solution explicitly using the above formalism, one recovers Eq. (3) with $a = (\mu - \lambda)/4$ and $c = \sqrt{3}(\mu + \lambda)/2$, which shows that the parameters μ and λ are simply rescaled phase parameters of the KPII equation: $\lambda = 2k_-$ and $\mu = 2k_+$. One can then check that this yields the correct relation between amplitude and velocity, namely Eq. (A8), which is equivalent to Eq. (A14).

2. Dressing of $h_0(a)$ and effects of spectral broadening in polychromatic SGs

In the context of the r-r and r-l bichromatic reductions of the kinetic equation the occupation functions (17) become

$$n^{\mathrm{r}}(a) = 2\pi \frac{F_1^{\mathrm{r}}\delta(a - a_1^{\mathrm{r}}) + F_2^{\mathrm{r}}\delta(a - a_2^{\mathrm{r}})}{a + F_1^{\mathrm{r}}\Delta^{\mathrm{co}}(a, a_1^{\mathrm{r}}) + F_2^{\mathrm{r}}\Delta^{\mathrm{co}}(a, a_2^{\mathrm{r}})}, \tag{A15a}$$

$$n^{\mathrm{l}}(a) = 0, \tag{A15b}$$

in the r-r case, and

$$n^{\mathrm{r}}(a) = 2\pi \frac{F_1^{\mathrm{r}}\delta(a - a_1^{\mathrm{r}})}{a + F_1^{\mathrm{r}}\Delta^{\mathrm{co}}(a, a_1^{\mathrm{r}}) + F_2^{\mathrm{l}}\Delta^{\mathrm{ct}}(a, a_2^{\mathrm{l}})}, \tag{A16a}$$

$$n^{\mathrm{l}}(a) = 2\pi \frac{F_2^{\mathrm{l}}\delta(a - a_2^{\mathrm{l}})}{a + F_1^{\mathrm{r}}\Delta^{\mathrm{ct}}(a, a_1^{\mathrm{r}}) + F_2^{\mathrm{l}}\Delta^{\mathrm{co}}(a, a_2^{\mathrm{l}})}, \tag{A16b}$$

in the r-l case. Moreover, since

$$|\Delta(a, a')| \to \infty \quad \text{as} \quad a \to a', \tag{A17}$$

for any admissible amplitude a', we have, e.g.,

$$\lim_{a\to a'} \frac{F_1^{\mathrm{r}}\Delta^{\mathrm{co}}(a, a')}{a + F_1^{\mathrm{r}}\Delta^{\mathrm{co}}(a, a') + F_2^{\mathrm{r}}\Delta^{\mathrm{co}}(a, a')} = 1, \tag{A18}$$

hence, we may evaluate the dressing of $h_0(a)$. First, in the r-r case, we have

$$h_0^{\mathrm{r,dr}}(a) = h_0(a) + h_0^{\mathrm{r,dr}}(a_1^{\mathrm{r}}) + h_0^{\mathrm{r,dr}}(a_2^{\mathrm{r}}), \tag{A19}$$

and by fixing either $a = a_1^{\mathrm{r}}$ and $a = a_2^{\mathrm{r}}$ we eventually find

$$h_0^{\mathrm{r,dr}}(a_1^{\mathrm{r}}) = -h_0(a_2^{\mathrm{r}}) = -4a_2^{\mathrm{r}}, \tag{A20a}$$

$$h_0^{\mathrm{r,dr}}(a_2^{\mathrm{r}}) = -h_0(a_1^{\mathrm{r}}) = -4a_1^{\mathrm{r}}. \tag{A20b}$$

Similarly, we have, in the r-l case

$$h_0^{\mathrm{r,dr}}(a_1^{\mathrm{r}}) = -h_0(a_2^{\mathrm{l}}) = -4a_2^{\mathrm{l}}, \tag{A21a}$$

$$h_0^{\mathrm{l,dr}}(a_2^{\mathrm{l}}) = -h_0(a_1^{\mathrm{r}}) = -4a_1^{\mathrm{r}}. \tag{A21b}$$

Ultimately, using these results, we can compute the horizontal covariance and the two-point correlation function, in order to recover Eqs. (21) and (22) of the main text.

As mentioned in Sec. V in the case of two-point correlations, the fact that the generated gas is not strictly polychromatic matters; to capture the associated effects of spectral broadening, instead of the delta-functional ansatz (7) we introduce

$$\tilde{f}^\alpha(a;x,y) = \sum_{i=1}^{M^\alpha} \frac{F_i^\alpha(x,y)}{\epsilon_g}\Theta\left(\frac{\epsilon_g}{2} - |a - a_i^\alpha|\right), \tag{A22}$$

where $\Theta(a)$ is the Heaviside function, such that $\int_{A^\alpha} \mathrm{d}a f^\alpha(a;x,y) = \int_{A^\alpha} \mathrm{d}a \tilde{f}^\alpha(a;x,y)$, $\forall\ (x,y)$. This spectral broadening becomes significant because two-point correlations have to be evaluated over sufficiently large scales, on which the gas cannot be considered homogeneous anymore. Over such large scales, the slight difference between the spectral parameter of a given soliton within the gas and the reference value a_i^α may translate, through the multiple scattering shifts it incurs, into a meaningful deviation from its reference trajectory $s^\gamma(a_i^\alpha) = x/y$. As such, we can define a "light cone" by computing the effective velocities $s_{i,-}^\gamma$ and $s_{i,+}^\gamma$ a soliton of amplitude $a_{i,-}^\alpha = a_i^\alpha - \epsilon_g/2$ and one of amplitude $a_{i,+}^\alpha = a_i^\alpha + \epsilon_g/2$ would have if they interacted with the polychromatic gas

$$s_{i,-}^\gamma = \frac{c(a_{i,-}^\gamma) - s_1^\alpha F_{1c}^\alpha \Delta(a_{i,-}^\gamma, a_1^\alpha) - s_2^\beta F_{2c}^\beta \Delta(a_{i,-}^\gamma, a_2^\beta)}{1 - F_{1c}^\alpha \Delta(a_{i,-}^\gamma, a_1^\alpha) - F_{2c}^\beta \Delta(a_{i,-}^\gamma, a_2^\beta)},$$

$$s_{i,+}^\gamma = \frac{c(a_{i,+}^\gamma) - s_1^\alpha F_{1c}^\alpha \Delta(a_{i,+}^\gamma, a_1^\alpha) - s_2^\beta F_{2c}^\beta \Delta(a_{i,+}^\gamma, a_2^\beta)}{1 - F_{1c}^\alpha \Delta(a_{i,+}^\gamma, a_1^\alpha) - F_{2c}^\beta \Delta(a_{i,+}^\gamma, a_2^\beta)}, \tag{A23}$$

where we assumed that modifying the amplitude of a single soliton from the gas by adding or subtracting $\epsilon_g/2$ does not significantly affect the weights of the two components of the bi-chromatic gas defined by Eqs. (16). The velocity of any soliton from the gas should verify $s_{i,-}^\gamma < s^\gamma(a;x,y) < s_{i,+}^\gamma$, which means that, given a known position x at which a soliton intersects with the horizontal at $y = 0$, the position at which it will intersect the horizontal at $y = Y$ is known with some uncertainty $\delta(Y,\epsilon_g) = |s_{i,+}^\gamma - s_{i,-}^\gamma|Y$. In the main text, when computing the two-point correlations (22), ϵ_g must be chosen to ensure that $\delta(Y,\epsilon_g) \ll Y$.

3. Numerical generation of stationary multisoliton KPII solutions

The numerical generation of N-soliton solutions adapted to approximate the stationary SG, for $N \gg 1$, relies on the Wronskian formulation (A2) where the function $\tau(x,y,t)$ is either given by (A12), for the Boussinesq equation, or (A10), for the KPII equation. In the latter case, it is more advantageous to consider the formulation $\tau = \det(K\,\mathrm{e}^\Theta G^T)$ than to adopt the Binet-Cauchy formula, that relies on the Van der Monde determinants (A10), as the number of nonzero minors increases exponentially with the number of solitons, making the algorithm unsuitable for the numerical study of solutions with $N \gg 1$. Note that, when it comes to the Boussinesq equation, in Eq. (A13) we have $C_j = (\mu_j - \lambda_j)\exp[-\frac{1}{2}(\mu_j - \lambda_j)x_{0j}]$, where x_{0j} is the ith soliton's positional phase parameter within N-soliton solution at $y = 0$ (for $N = 1$ this gives the position of the maximum of the isolated line soliton at $y = 0$).

As previously discussed, stationary solutions of the Galilean-boosted KPII equation can be identified with solutions of the Boussinesq equation. To this end, the map between the two expressions of $\tau(x,y,t=0)$, for the Boussinesq and KPII equations, is detailed below. The matrix G in (A10) can generically be put in the form

$$G = \begin{pmatrix} g_{1,1} & g_{1,2} & 0 & 0 & \cdots & 0 & 0 \\ 0 & 0 & g_{2,3} & g_{2,4} & \cdots & 0 & 0 \\ \vdots & \vdots & \vdots & \vdots & \ddots & \vdots & \vdots \\ 0 & 0 & \cdots & \cdots & 0 & g_{N,2N-1} & g_{N,2N} \end{pmatrix}, \tag{A24}$$

and, comparing (A10) with (A13), we obtain the map,

$$g_{n,2n} = -c_n \frac{g_{n,2n-1}}{\mu_n - \lambda_n} \prod_{n \neq m} \frac{\lambda_n - \lambda_m}{\mu_n - \lambda_m}, \tag{A25}$$

where $c_n = \lambda_n - \mu_n$. Without loss of generality, we can assume $g_{n,2n-1} = 1$ for $n = 1, 2 \ldots N-1$ and the element $g_{N,2N-1}$ is given by

$$g_{N,2N-1} = \prod_{n=N}^{1} \prod_{m=1}^{n-1} \mathrm{sgn}(\lambda_n - \lambda_m). \tag{A26}$$

Note that, once the map is established, the solutions generated by the two different algorithms are identical, see Fig. 5.

As is the case with the schemes for the numerical construction of the N-soliton solution for NLS and KdV using the Darboux transformation [66,71], this algorithm is subject to round-off errors during summation of exponentially small and large values. Following the procedure developed in [71], high-precision arithmetic routines have been implemented to overcome the numerical accuracy problems.

[1] V. E. Zakharov, Kinetic equation for solitons, Sov. Phys. JETP **33**, 538 (1971).

[2] G. A. El, The thermodynamic limit of the Whitham equations, Phys. Lett. A **311**, 374 (2003).

[3] G. A. El and A. M. Kamchatnov, Kinetic equation for a dense soliton gas, Phys. Rev. Lett. **95**, 204101 (2005).
[4] G. El and A. Tovbis, Spectral theory of soliton and breather gases for the focusing nonlinear Schrödinger equation, Phys. Rev. E **101**, 052207 (2020).
[5] T. Congy, G. El, and G. Roberti, Soliton gas in bidirectional dispersive hydrodynamics, Phys. Rev. E **103**, 042201 (2021).
[6] A. Costa, A. R. Osborne, D. T. Resio, S. Alessio, E. Chrivì, E. Saggese, K. Bellomo, and C. E. Long, Soliton turbulence in shallow water ocean surface waves, Phys. Rev. Lett. **113**, 108501 (2014).
[7] I. Redor, E. Barthélemy, H. Michallet, M. Onorato, and N. Mordant, Experimental evidence of a hydrodynamic soliton gas, Phys. Rev. Lett. **122**, 214502 (2019).
[8] P. Suret, A. Tikan, F. Bonnefoy, F. Copie, G. Ducrozet, A. Gelash, G. Prabhudesai, G. Michel, A. Cazaubiel, E. Falcon, G. El, and S. Randoux, Nonlinear spectral synthesis of soliton gas in deep-water surface gravity waves, Phys. Rev. Lett. **125**, 264101 (2020).
[9] T. Leduque, E. Barthélemy, H. Michallet, J. Sommeria, and N. Mordant, Space–time statistics of 2D soliton gas in shallow water studied by stereoscopic surface mapping, Exp. Fluids **65**, 84 (2024).
[10] G. Marcucci, D. Pierangeli, A. J. Agranat, R.-K. Lee, E. DelRe, and C. Conti, Topological control of extreme waves, Nat. Commun. **10**, 5090 (2019).
[11] S. Mossman, G. C. Katsimiga, S. I. Mistakidis, A. Romero-Ros, T. M. Bersano, P. Schmelcher, P. G. Kevrekidis, and P. Engels, Observation of dense collisional soliton complexes in a two-component Bose-Einstein condensate, Commun. Phys. **7**, 163 (2024).
[12] M. J. Ablowitz and H. Segur, *Solitons and the Inverse Scattering Transform* (SIAM, Philadelphia, 1981)
[13] S. Novikov, S. Manakov, L. Pitaevskii, and V. E. Zakharov, *Theory of Solitons: The Inverse Scattering Method* (Springer Science & Business Media, 1984).
[14] V. E. Zakharov, Turbulence in integrable systems, Stud. Appl. Math. **122**, 219 (2009).
[15] P. Suret, M. Dufour, G. Roberti, G. El, F. Copie, and S. Randoux, Soliton refraction by an optical soliton gas, Phys. Rev. Res. **5**, L042002 (2023).
[16] L. Fache, F. Bonnefoy, G. Ducrozet, F. Copie, F. Novkoski, G. Ricard, G. Roberti, E. Falcon, P. Suret, G. El *et al.*, Interaction of soliton gases in deep-water surface gravity waves, Phys. Rev. E **109**, 034207 (2024).
[17] G. A. El, Soliton gas in integrable dispersive hydrodynamics, J. Stat. Mech. (2021) 114001.
[18] P. Suret, S. Randoux, A. Gelash, D. Agafontsev, B. Doyon, and G. El, Soliton gas: Theory, numerics and experiments, Phys. Rev. E **109**, 061001 (2024).
[19] O. A. Castro-Alvaredo, B. Doyon, and T. Yoshimura, Emergent hydrodynamics in integrable quantum systems out of equilibrium, Phys. Rev. X **6**, 041065 (2016).
[20] B. Bertini, M. Collura, J. De Nardis, and M. Fagotti, Transport in out-of-equilibrium XXZ chains: Exact profiles of charges and currents, Phys. Rev. Lett. **117**, 207201 (2016).
[21] B. Doyon, Lecture notes on generalised hydrodynamics, SciPost Phys. Lecture Notes 18 (2020).
[22] H. Spohn, *Hydrodynamic Scales of Integrable Many-Body Systems* (World Scientific, Singapore, 2023).
[23] T. Bonnemain, B. Doyon, and G. El, Generalized hydrodynamics of the KdV soliton gas, J. Phys. A: Math. Theor. **55**, 374004 (2022).
[24] T. Bonnemain and B. Doyon, Soliton gas of the integrable Boussinesq equation and its generalised hydrodynamics, arXiv:2402.08669.
[25] B. Doyon and T. Yoshimura, A note on generalized hydrodynamics: Inhomogeneous fields and other concepts, SciPost Phys. **2**, 014 (2017).
[26] J. E. Zhang and Y. Li, Bidirectional solitons on water, Phys. Rev. E **67**, 016306 (2003).
[27] D. J. Kaup, A higher-order water-wave equation and the method for solving It, Prog. Theor. Phys. **54**, 396 (1975).
[28] J.-H. Lee, O. Pashaev, C. Rogers, and W. Schief, The resonant nonlinear Schrödinger equation in cold plasma physics. Application of Bäcklund–Darboux transformations and superposition principles, J. Plasma Phys. **73**, 257 (2007).
[29] J. Boussinesq, Théorie des ondes et des remous qui se propagent le long d'un canal rectangulaire horizontal, en communiquant au liquide contenu dans ce canal des vitesses sensiblement pareilles de la surface au fond, J. Mathématiques Pures et Appliquées **17**, 55 (1872).
[30] L. Dieli, D. Pierangeli, E. DelRe, and C. Conti, Observation of two-dimensional dam break flow and a gaseous phase of solitons in a photon fluid, Phys. Rev. Lett. **133**, 183801 (2024).
[31] B. B. Kadomtsev and V. I. Petviashvili, On the stability of solitary waves in weakly dispersing media, Sov. Phys. Dokl. **15**, 539 (1970).
[32] Y. Kodama, *Solitons in Two-Dimensional Shallow Water* (SIAM-Society for Industrial and Applied Mathematics, Philadelphia, 2018).
[33] M. S. Ruderman, Kadomtsev-Petviashvili equation for magnetosonic waves in Hall plasmas and soliton stability, Phys. Scr. **95**, 095601 (2020).
[34] S. K. Turitsyn and G. E. Fal'kovich, Stability of magnetoelastic solitons and self-focusing of sound in antiferromagnets, Sov. Phys. JETP **62**, 146 (1985).
[35] G. Huang, V. A. Makarov, and M. G. Velarde, Two-dimensional solitons in Bose-Einstein condensates with a disk-shaped trap, Phys. Rev. A **67**, 023604 (2003).
[36] A. M. Kamchatnov and L. P. Pitaevskii, Stabilization of solitons generated by a supersonic flow of Bose-Einstein condensate past an obstacle, Phys. Rev. Lett. **100**, 160402 (2008).
[37] M. A. Hoefer and B. Ilan, Dark solitons, dispersive shock waves, and transverse instabilities, SIAM Multiscale Model. Sim. **10**, 306 (2012).
[38] G. Biondini and Y. Kodama, On a family of solutions of the Kadomtsev–Petviashvili equation which also satisfy the Toda lattice hierarchy, J. Phys. A: Math. Gen. **36**, 10519 (2003).
[39] G. Biondini and S. Chakravarty, Soliton solutions of the Kadomtsev-Petviashvili II equation, J. Math. Phys. **47**, 033514 (2006).
[40] G. Biondini, Line soliton interactions of the Kadomtsev-Petviashvili equation, Phys. Rev. Lett. **99**, 064103 (2007).
[41] Y. Kodama, Young diagrams and N-soliton solutions of the KP equation, J. Phys. A: Math. Gen. **37**, 11169 (2004).
[42] Y. Kodama, *KP Solitons and the Grassmannians: Combinatorics and Geometry of Two-Dimensional Wave Patterns* (Springer, New York, 2017), Vol. 22.

[43] H. McKean, Boussinesq's equation on the circle, Commun. Pure Appl. Math. **34**, 599 (1981).
[44] R. Courant and K. O. Friedrichs, *Supersonic Flow and Shock Waves* (Springer-Verlag, Berlin, 1948).
[45] L. Landau and E. Lifshitz, *Fluid Mechanics* (Elsevier Science, Amsterdam, 2013), Vol. 6.
[46] G. B. Whitham, *Linear and Nonlinear Waves* (John Wiley & Sons, Hoboken, NJ, 2011).
[47] G. A. El, A. Gammal, and A. M. Kamchatnov, Oblique dark solitons in supersonic flow of a Bose-Einstein condensate, Phys. Rev. Lett. **97**, 180405 (2006).
[48] G. A. El, A. M. Kamchatnov, V. V. Khodorovskii, E. S. Annibale, and A. Gammal, Two-dimensional supersonic nonlinear Schrödinger flow past an extended obstacle, Phys. Rev. E **80**, 046317 (2009).
[49] M. A. Hoefer, G. A. El, and A. M. Kamchatnov, Oblique spatial dispersive shock waves in nonlinear Schrödinger Flows, SIAM J. Appl. Math. **77**, 1352 (2017).
[50] N. Freeman and J. Nimmo, Soliton solutions of the Korteweg de Vries and the Kadomtsev-Petviashvili equations: The Wronskian technique, Proc. R. Soc. London. A. Math. Phys. Sci. **389**, 319 (1983).
[51] R. Hirota, *The Direct Method in Soliton Theory*, 155 (Cambridge University Press, Cambridge, 2004).
[52] L. Bogdanov and V. Zakharov, The Boussinesq equation revisited, Physica D **165**, 137 (2002).
[53] F. Lambert, M. Musette, and E. Kesteloot, Soliton resonances for the good Boussinesq equation, Inverse Probl. **3**, 275 (1987).
[54] G. A. El, A. Kamchatnov, M. V. Pavlov, and S. Zykov, Kinetic equation for a soliton gas and its hydrodynamic reductions, J. Nonlinear Sci. **21**, 151 (2011).
[55] T. Congy, H. T. Carr, G. Roberti, and G. A. El, Riemann problem for polychromatic soliton gases: A testbed for the spectral kinetic theory, arXiv:2405.05166.
[56] M. D. Maiden, D. V. Anderson, N. A. Franco, G. A. El, and M. A. Hoefer, Solitonic dispersive hydrodynamics: Theory and observation, Phys. Rev. Lett. **120**, 144101 (2018).
[57] P. Sprenger, M. A. Hoefer, and G. A. El, Hydrodynamic optical soliton tunneling, Phys. Rev. E **97**, 032218 (2018).
[58] G. Biondini, S. Li, and D. Mantzavinos, Soliton trapping, transmission, and wake in modulationally unstable media, Phys. Rev. E **98**, 042211 (2018).
[59] G. Biondini and J. Lottes, Nonlinear interactions between solitons and dispersive shocks in focusing media, Phys. Rev. E **99**, 022215 (2019).
[60] K. van der Sande, G. A. El, and M. A. Hoefer, Dynamic soliton–mean flow interaction with non-convex flux, J. Fluid Mech. **928**, A21 (2021).
[61] A. Mucalica and D. E. Pelinovsky, Solitons on the rarefaction wave background via the Darboux transformation, Proc. R. Soc. A **478**, 20220474 (2022).
[62] M. J. Ablowitz, J. T. Cole, G. A. El, M. A. Hoefer, and X.-D. Luo, Soliton–mean field interaction in Korteweg–de Vries dispersive hydrodynamics, Stud. Appl. Math. **151**, 795 (2023).
[63] B. Rozhdestvenskii and N. Janenko, *Systems of Quasilinear Equations and Their Applications to Gas Dynamics* (American Mathematical Society, Providence, RI, 1983).
[64] F. Carbone, D. Dutykh, and G. A. El, Macroscopic dynamics of incoherent soliton ensembles: Soliton gas kinetics and direct numerical modelling, Europhys. Lett. **113**, 30003 (2016).
[65] B. Doyon, Exact large-scale correlations in integrable systems out of equilibrium, SciPost Phys. **5**, 054 (2018).
[66] T. Congy, G. A. El, G. Roberti, and A. Tovbis, Dispersive hydrodynamics of soliton condensates for the Korteweg–de Vries equation, J. Nonlinear Sci. **33**, 104 (2023).
[67] A. Toffoli, M. Onorato, A. R. Osborne, and J. Monbaliu, Non-Gaussian properties of shallow water waves in crossing seas, in *Extreme Ocean Waves*, edited by E. Pelinovsky and C. Kharif (Springer International Publishing, Cham, 2016), pp. 75–91.
[68] J. Nimmo and N. Freeman, A method of obtaining the N-soliton solution of the Boussinesq equation in terms of a wronskian, Phys. Lett. A **95**, 4 (1983).
[69] J. W. Miles, Diffraction of solitary waves, Z. Angew. Math. Phys. **28**, 889 (1977).
[70] E. Medina, An N soliton resonance solution for the KP equation: Interaction with change of form and velocity, Lett. Math. Phys. **62**, 91 (2002).
[71] A. A. Gelash and D. S. Agafontsev, Strongly interacting soliton gas and formation of rogue waves, Phys. Rev. E **98**, 042210 (2018).